Biochemical and Biophysical Research Communications 374 (2008) 28–32

Contents lists available at ScienceDirect

Biochemical and Biophysical Research Communications

journal homepage: www.elsevier.com/locate/ybbrc

3D local structure around Zn in Kti11p as a representative Zn-(Cys)4 motif as obtained by MXAN

Meijuan Yu [a], Feifei Yang [a], Wangsheng Chu [a,*], Yu Wang [a,b], Haifeng Zhao [a], Bin Gao [a,c], Wei Zhao [d], Jianping Sun [d], Fangming Wu [d], Xiaowei Zhang [e], Yunyu Shi [d], Ziyu Wu [a,b,f,*]

[a] Institute of High Energy Physics, Chinese Academy of Sciences, Beijing Synchrotron Radiation Facility, 19B YuquanLu, Shijingshan District, Beijing 100049, China
[b] National Synchrotron Radiation Laboratory, University of Science and Technology of China, Hefei 230026, China
[c] Theoretical Chemistry, Royal Institute of Technology, Sweden
[d] Hefei National Laboratory for Physical Sciences at Microscale and School of Life Sciences, University of Science and Technology of China, Hefei, Anhui 230027, China
[e] State Key Laboratory of Medical Genomics, Shanghai Institute of Hematology, Rui Jin Hospital, School of Medicine, Shanghai Jiao Tong University, Shanghai 200025, China
[f] Theoretical Physics Center for Science Facilities, Chinese Academy of Sciences, Beijing 100049, China

ARTICLE INFO

Article history:
Received 15 June 2008
Available online 9 July 2008

Keywords:
Zinc motif
Kti11p
EXAFS
XANES
Fingerprints
MXAN

ABSTRACT

Zinc is an important component of many proteins that play key roles in transcription, translation, and catalysis. Kti11p, DESR1, both belonging to a protein family characterized by a CSL zinc finger domain, and the co-catalytic zinc–protein PML containing a Zn^{2+} binding domain called RING or C_3HC_4 finger are all structurally determined by NMR although the zinc sites are silent to this spectroscopical method. The comparison of X-ray absorption near-edge spectroscopy (XANES) data for the three proteins demonstrates that fingerprints effect is a reliable method for a primary characterization of ligand species. A*b initio* full MS calculations performed by MXAN are applied to obtain chemical and stereo structural information around the Zn ion in Kti11p. For the first time this high-spatial resolution technique confirms the formation of a stable Zn tetrahedral configuration with four sulfur ligands, and returns extremely accurate bond angle information between ligands.

It is well known that Zn-proteins play important roles in many biological processes, such as transcription, translation and catalysis [1,2]. These functions depend on the subtle structures around the metal ions, including the ligand species and coordination geometry. However, limited structural information is available, mainly because Zn ion is silent to standard spectroscopical techniques used to characterize proteins such as nuclear magnetic resonance (NMR) and electron spin resonance (ESR). Zn is usually coordinated with N, O, and S atoms of His, Asp, and/or Cys ligands and there are three kinds of Zn motifs with different ligands and coordination geometries: (i) catalytic, (ii) co-catalytic, and (iii) structural [3,4].

Based on the above description, a site-selective, high-spatial resolution technique is needed to reconstruct the local stereo structures around the metal ions, including ligand species and coordination geometries, in order to identify a correlation with biological functions. X-ray diffraction and NMR are widely used methods capable to resolve the protein structures. However, at low resolutions they are not capable to obtain subtle information of the local structures. Moreover, different from other transition metals such as copper, iron, manganese, and cobalt, zinc is silent to NMR for its full electron 3d-shell. However, X-ray absorption spectroscopy (XAS) is a technique associated to single and multiple scattering processes in a local cluster around the photoabsorber atom. Thus it is really a powerful method to provide high-spatial resolution structural information combined to partial and local Density of State information. It has also limited experimental demands and may investigate samples in solutions, as powders or crystals [5–13].

Kti11p is a small, highly conserved CSL zinc finger-containing protein found in many eukaryotes [14]. It was identified as one of the factors required to confer sensitivity of *Saccharomyces cerevisiae* to *Kluyveromyces lactis* zymocin [15,16]. Kti11p is an important protein for the synthesis of diphthamide, the target of diphtheria toxin and *Pseudomonas* exotoxin A [17]. Disruption and mutagenesis of *KTI11p* will result in the *tot* phenotype, including zymocin resistance [16].

Several investigations of Kti11p were performed, but its structure was unsolved until recent NMR results were published [14]. For its novel structure it was suggested that Kti11p may represent a new form of the zinc ribbon fold group in the zinc fingers database [18]. However, as addressed before, no definite Zn position was identified by NMR. EXAFS data of the Zn K-edge of Kti11p showed that Kti11p contains a $Zn(Cys)_4$ motif, in which four con-

* Corresponding authors. Fax: +86 01 88235294.
E-mail addresses: cws@ihep.ac.cn (W. Chu), wuzy@ihep.ac.cn (Z. Wu).

0006-291X/$ - see front matter © 2008 Elsevier Inc. All rights reserved.
doi:10.1016/j.bbrc.2008.06.116

served cysteine residues coordinate with a single zinc ion in a tetrahedral configuration [14].

EXAFS is a well-recognized method capable to determine accurate bond distances and coordination numbers in different systems and conditions. It supported the numerical reconstruction of many complex systems [11,19,20]. However, when compared to XANES spectroscopy it has a high demand of signal-to-noise ratio. Besides, it is not sensitive to the stereo structure and the chemical nature when dealing with biological systems [21]. However, the fingerprints capability of XANES easily supplies direct information of coordinated atomic species and configurations. Furthermore, thanks to the contribution of multiple scattering processes in this range, a new package named MXAN, based on a XANES quantitative analysis sensitive to bond angles, species of ligands and geometries, was successfully applied to a large number of complex systems [8,10,22]. It returns the 3D structures which are certainly correlated with functions and activities of biological systems.

As mentioned by Clark-Baldwin et al., there are XANES differences occurring in different types of ligands around zinc such as S_4, S_3N, S_2N_2, but they could not be distinguished in organic system as easily as in different inorganic models [23]. Combining experimental data of other proteins such as the homologous protein DESR1 [24], and the co-catalytic zinc–protein PML containing a Zn ion binding domain called RING or C_3HC_4 finger [25], we demonstrate how XANES fingerprints effect may differentiate different zinc motifs in proteins like what mentioned by Clark-Baldwin et al. Furthermore, using the novel software package MINUIT XANES (MXAN) in the framework of the *ab initio* full multiple scattering (MS) theory, previously tested on other biological structures [21,26–31], a quantitative analysis has been performed on Kti11p.

Materials and methods

Cloning, expression and purification of Kti11p have been previously reported [14]. *KTI11* from *S. cerevisiae* S288C was cloned into a pET-28a(+) expression vector (Novagen) to give an N-terminal methionine followed by a valine and a 6×His tag at its C terminus. It was then rebuilt to *Escherichia coli* BL21 (DE3) Gold (Stratagene) host cells, which was induced when $A_{600} = 1.0$ in M9 medium. 1 mM IPTG and 20 μM $ZnSO_4$ were added at 16 °C for 20 h for the expression. Purification was done by a Nickel-Chelating Sepharose Fast Flow (Amersham Pharmacia Biotech). Then the sample was filtered in a HiLoad 16/60 Superdex 75 with an HPLC system (Amersham Pharmacia Biotech). The use of SDS–PAGE supported the purity of the protein and BCA kits (Pierce) were employed to measure the sample concentration.

XAS measurements were performed at the X-ray absorption station of the beamline 4W1B at the Beijing synchrotron radiation facility (BSRF). The typical energy of the storage ring was 2.2 GeV with a current decreasing from 120 to 80 mA during experiments. Data were collected in the "fluorescence yield" (FY) mode using a Si (1 1 1) double crystal monochromator.

To minimize the higher harmonics content, a detuning of 30% of the monochromator crystals was performed. An ionization chamber flowed by 25% argon and 75% nitrogen was used to monitor the incident beam intensity (I_0), and a Lytle detector flowed by argon was used to record the fluorescence signal (I_f). To ensure the liability of the experiment, both solution and powder samples were measured consecutively twice. The solution was kept in a cell sealed by Kapton films and with a Teflon spacer of 1.2 mm. Freeze-dried powder sample was pressed into a sheet to get a well-proportioned distribution for a better signal-to-noise ratio. No changes among consecutive XAS spectra of each sample have been detected. Furthermore, samples measured in different states exhibit the same behavior suggesting that radiation damage is absent or negligible for these experiments with monochromatic radiation and no changes of the local structure around the metal ion of this protein have been observed.

Results

XANES fingerprints

Looking at the XAS spectrum of Kti11p (Fig. 1), five features are easily recognized in the spectrum. The first three peaks: A, B, and C are produced by the photoelectrons excited in the first atomic shell, due to MS resonances. As a consequence they have a strong affinity with both geometry and species existing in the first atomic coordination.

Besides, a comparison between XANES spectra of Ki11p, its homologous protein DESR1 and the co-catalytic PML protein was also made. Kti11p and DESR1 both have a Zn ion coordinated with four sulphur atoms in a tetrahedral geometry, while PML has two zinc sites one of which is coordinated by three sulphur atoms and one nitrogen atom [24,25]. It is obvious that only minor differences are detectable in the XANES spectra of the PML protein around the feature B, the amplitude of which is relatively lower than that in others. A similar behavior is detectable for the feature B_1 in the difference spectra of Kti11p with DESR1 and PML. It could be assigned to the nitrogen atom in one of the zinc motifs in PML, which shows a good correspondence with what mentioned by Clark-Baldwin et al. [23]. Actually, our work confirms the reliability of the XANES fingerprints technique to identify specific metal local structures in proteins belonging to the same series.

MXAN calculations

MXAN (MINUIT XANES) is a software package capable to perform a quantitative analysis of a XANES spectrum from the absorption edge up to about 200 eV. It can extract detailed structural information around the zinc ion site via a comparison of experimental data and theoretical calculations generated by changing relevant geometrical parameters of the atomic sites [32–34]. This package searches for a minimum of the square residue function in the space of the parameters defined as:

$$S^2 = n\frac{\sum_{i=1}^{w_i}[(y_i^{\mathrm{th}} - y_i^{\mathrm{exp}})\varepsilon_i^{-1}]^2}{\sum_{i=1}^{m} w_i} \quad (1)$$

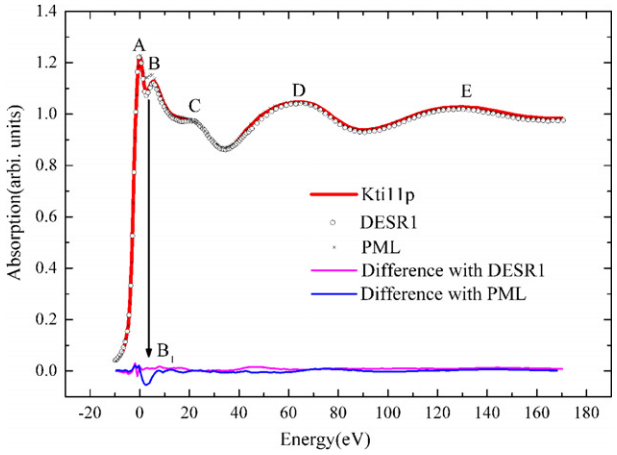

Fig. 1. Comparison between Zn K-edge XANES of: Kti11p protein, its homologous DESR1 and the co-catalytic PML. The magenta and the blue lines at the bottom of this figure outline differences for Kti11p with DESR1 and PML (Kti11p-DESR1, Kti11p-PML), respectively.

which is an important criterion to evaluate the result. In Eq. (1), n is the number of independent parameters, m is the number of data points, y_i^{th} and y_i^{exp} are the theoretical and experimental absorption values respectively, ε_i is the individual error in the experimental data set and w_i is a statistical weight. When $w_i = constant = 1$, the square residual function S^2 reduces to the statistical χ^2 function. The X-ray absorption cross-sections have been calculated using the full multiple scattering scheme in the framework of the muffin-tin (MT) approximation for the shape of the potential [35,36]. In this case, the exchange and the correlation part of the potential have been determined on the basis of the local density approximation of the self-energy. Inelastic processes were accounted for by a convolution with a broadening Lorentzian function having an energy-dependent width of the form $\Gamma(E) = \Gamma_c + \Gamma_{mfp}(E)$. The constant part Γ_c accounts for both the core–hole lifetime (1.8 eV) [37] and the experimental resolution (1.5 eV), while the energy-dependent term represents all the intrinsic and extrinsic inelastic processes [22,32,38]. The MT radii were chosen according to the Norman criterion with a 15% overlap [39,40]. Essentially, the influence of these non-structural parameters will result in an increase of a few percentages of the error value in the structural parameters' determination. The method takes into account MS events in a rigorous way through the evaluation of the scattering path operator [35,41] and its reliability has been successfully tested over the years in many different applications [22,32,42,43].

According to one structural model of Kti11p in the Protein Data Bank, a cluster containing 39 atoms within 5.3 Å from the zinc ion has been chosen for further analysis (see details in Supplementary Material). S^2 for the initial model is 7.3 (Fig. 2A). According to Eq. (1), XANES reproduced by initial model did not have a good consistent with the experimental data.

We defined four ligands according to the local structure with four nearest sulphur atoms and each Cys residue was allowed to move rigidly with the sulphur atom they contained. For each ligand the bond distance R and the two angles θ and Φ of the polar coordinates were allowed to search for the optimized position [44]. The initial values of these parameters from the chosen model are listed in Tables 1 and 2. However, the angles θ and Φ of the ligand1, i.e. Cys26, were fixed to prevent unphysical displacement of the four ligands. The position of the ligand1 has been also used as the reference system of the other displacements. The best fit achieved by MXAN is compared with the experimental data with S^2 of 2.2 (Fig. 2B). MXAN distances are listed (Table 1) together with the EXAFS parameters supplied by Sun et al. [14] and θ and Φ of the four main ligands as available by XANES are listed in Table 2. The error bars for all parameters obtained by MXAN are also showed according to the best file provided by MXAN. The error values presented in Tables 1 and 2 include the influence of those non-structural parameters defined in MXAN and the correlation between these structural parameters [8,27,45]. The distances returned by MXAN and EXAFS are in excellent agreement, addressing a relevant consistency between these two XAS contributions one associated to SS scattering contributions and the other sensitive to MS paths. The revised Zn local structure of Kti11p is outlined in Fig. 3. A compact tetrahedral geometry is stable enough to avoid other atoms or molecules such as water to enter. It may explain why this particular kind of protein, characterized by a compact structural Zn site, does not show catalytic activities.

Table 2
Comparison of θ and Φ angles for the four conserved cysteine residues of the PDB with MXAN data

		Cys26-Pro27	Cys28-Gly29	Cys48	Cys51-Ser50-Ser52
θ	PDB	−33.8	158.4	77.4	228.7
	MXAN	−33.8	172.4 ± 8.0	68.4 ± 7.0	245.3 ± 5.0
Φ	PDB	118.3	134.4	62.1	40.3
	MXAN	118.3	129.7 ± 6.7	68.7 ± 6.2	43.7 ± 5.0

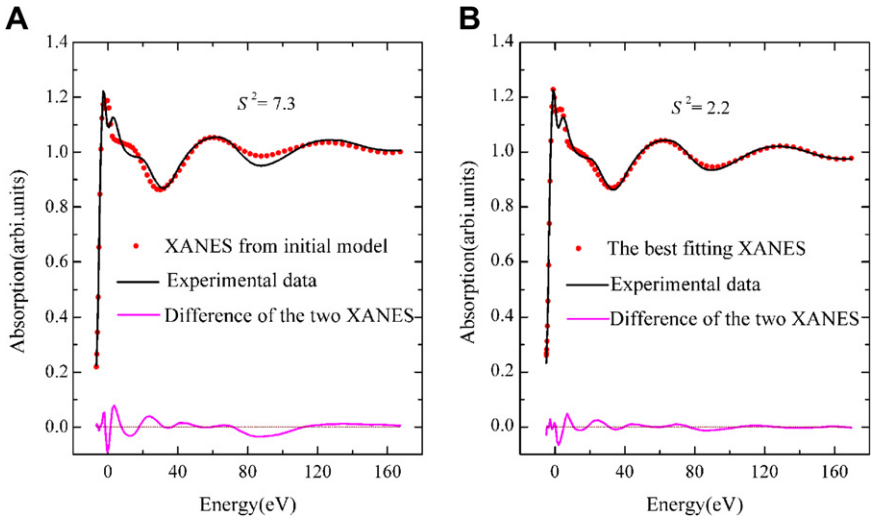

Fig. 2. Comparison of Zn K-edge XANES experimental data of Kti11p with simulations obtained with the parameters of the initial model (A) and best fit results (B). At each figure of the bottom the difference between the XANES spectra.

Table 1
Comparison of the distances between the Zn^{2+} and the four S atoms from the four conserved cysteine residues as obtained by PDB, EXAFS, and XANES

	Zn-SG (Cys26) (Å)	Zn-SG (Cys28) (Å)	Zn-SG (Cys48) (Å)	Zn-SG (Cys51) (Å)
PDB	2.18	2.28	2.32	2.42
EXAFS	2.31	2.31	2.31	2.31
XANES	2.30 ± 0.02	2.29 ± 0.02	2.30 ± 0.02	2.29 ± 0.02

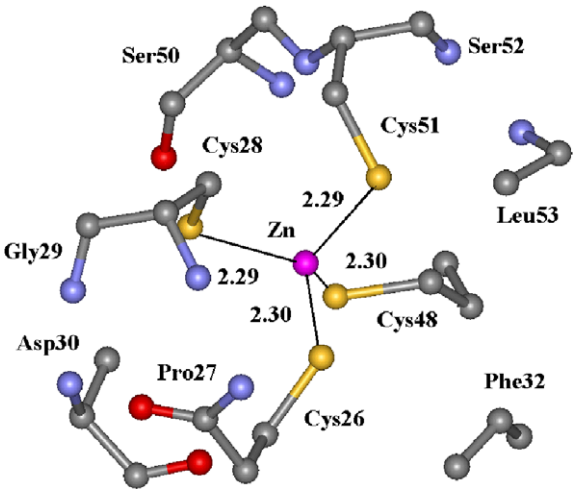

Fig. 3. The local structure around the Zn ion in the Kti11p as obtained by MXAN. Sulfur, carbon, nitrogen, and oxygen atoms are yellow, grey, blue, and red spheres, respectively. The four thin solid lines refer to the four S bond distances around the Zn ion. (For interpretation of the references in colour in this figure legend, the reader is referred to the web version of this article.)

Discussion

The subtle differences of spectra for the experimental data and the best fitting result in Fig. 2B occur in the region of feature B and C just above the absorption edge. Their origin may be associated to small changes of the potential probed by the photoelectrons. Actually, in this energy region just above the absorption edge, the relatively low energy of the photoelectron and its long mean free path make it extremely sensitive to details of the potential. Due to the muffin-tin approximation used in our simulations [35,36], it is difficult to reproduce an accurate potential in the low energy region. However, the results obtained already represent a significant improvement and better support the understanding of biological processes in which the Kti11p protein is involved.

Above all, with the advent of *ab initio* full multiple scattering (MS) method, new possibilities emerge for accurate structural analysis and, in particular, new packages such as MXAN allow dealing much more complex structural problems. Combining the unique XANES fingerprints capabilities and accurate computational tools such as MXAN important structural reconstructions can be achieved as showed in this contribution. It represents not only a convenient way for biologists to identify specific Zn local structures and reconstruct them with high accuracy, but a significant progress in an area where these information can be really useful for other researches such as those addressing the chemical processes involving these important biological systems.

Acknowledgments

Sincere thanks are due to A. Marcelli and M. Benfatto for many helpful discussions. Sincere thanks are also due to Z. Chen for his support to this work. This work was supported by the National Outstanding Youth Fund (Project No. 10125523 to Z.W.), the Key Important Project of the National Natural Science Foundation of China (N. 10490190 and 10490191) and the Knowledge Innovation Program of the Chinese Academy of Sciences (KJCX2-SW-N11).

Appendix A. Supplementary data

Supplementary data associated with this article can be found, in the online version, at doi:10.1016/j.bbrc.2008.06.116.

References

[1] S.J. Lippard, J.M. Berg, Principles of Bioinorganic Chemistry, University Science Books, Sausalito, 1994.
[2] H.A.O. Hill, P.J. Sadler, A.J. Thomsonm, Metal Sites in Proteins and Models, Springer, Berlin, 1999.
[3] B.L. Vallee, D.S. Auld, Zinc coordination function and structure of zinc enzymes and other proteins, Biochemistry 29 (1990) 5647.
[4] B.L. Vallee, D.S. Auld, Zinc: biological functions and coordination motifs, Acc. Chem. Res. 26 (1993) 543.
[5] S.S. Hasnain, K.O. Hodgson, Structure of metal centres in proteins at subatomic resolution, J. Synchrotron Radiat. 6 (1999) 852–864.
[6] S.S. Hasnain, R.W. Strange, Marriage of XAFS and crystallography for structure–function studies of metalloproteins, J. Synchrotron Radiat. 10 (2003) 9–15.
[7] L. Banci, I. Bertini, S. Ciofi-Bafoni, E. Katsari, N. Katsaros, K. Kubicek, S. Mangani, A copper(I) protein possibly involved in the assembly of Cu_A center of bacterial cytochrome *c* oxidase, Proc. Natl. Acad. Sci. 102 (2005) 3994–3999.
[8] S. Della Longa, A. Arcovito, M. Girasole, J.L. Hazemann, M. Benfatto, Quantitative analysis of X-ray absorption near edge structure data by a full multiple scattering procedure: The Fe–CO geometry in photolyzed carbonmonoxy-myoglobin single crystal, Phys. Rev. Lett. 87 (2001) 155501.
[9] S. Della Longa, A. Arcovito, M. Benfatto, A. Congiu-Castellano, M. Girasole, J.L. Hazemann, A. Lo Bosco, Redox-induced structural dynamics of Fe–heme ligand in myoglobin by X-ray absorption spectroscopy, Biophys. J. 85 (2003) 549–558.
[10] M. Benfatto, S. Della Longa, C.R. Natoli, The MXAN procedure: a new method for analysing the XANES spectra of metalloproteins to obtain structural quantitative information, J. Synchrotron Radiat. 10 (2003) 51–57.
[11] S.D. Conradson, B.K. Burgess, W.E. Newton, A.D. Cicco, A. Filipponi, Z.Y. Wu, C.R. Natoli, B. Hedman, K.O. Hodgson, Selenol binds to iron in nitrogenase iron–molybdenum cofactor: an extended X-ray absorption fine structure study, Proc. Natl. Acad. Sci. 91 (1994) 1290–1293.
[12] K.L. Stone, R.K. Behan, M.T. Green, X-ray absorption spectroscopy of chloroperoxidase compound I: insight into the reactive intermediate of P450 chemistry, Proc. Natl. Acad. Sci. 102 (2005) 16563–16565.
[13] M.C. Feiters, A.P.A.M. Eijkelenboom, H.-F. Nolting, B. Krebs, F.M.I. van den Ent, R.H.A. Plasterk, R. Kaptein, R. Boelens, X-ray absorption spectroscopic studies of zinc in the N-terminal domain of HIV-2 integrase and model compounds, J. Synchrotron Radiat. 10 (2003) 86–95.
[14] J. Sun, J. Zhang, F. Wu, C. Xu, S. Li, W. Zhao, Z. Wu, J. Wu, C.Z. Zhou, Y. Shi, Solution structure of Kti11p from *Saccharomyces cerevisiae* reveals a novel zinc-binding module, Biochemistry 44 (2005) 8801–8809.
[15] A.R. Butler, J.H. White, Y. Folawiyo, A. Edlin, D. Gardiner, M.J.R. Stark, Two *Saccharomyces cerevisiae* genes which control sensitivity to G1 arrest induced by *Kluyveromyces lactis* toxin, Mol. Cell. Biol. 14 (1994) 6306–6316.
[16] L. Fichtner, R. Schaffrath, KTI11 and KTI13 *Saccharomyces cerevisiae* genes controlling sensitivity to G1 arrest induced by *Kluyveromyces lactis* zymocin, Mol. Microbiol. 44 (2002) 865–875.
[17] S. Liu, S.H. Leppla, Retroviral insertional mutagenesis identifies a small protein required for synthesis of diphthamide, the target of bacterial ADP-ribosylating toxins, Mol. Cell 12 (2003) 603–613.
[18] S.S. Krishna, I. Majumdar, N.V. Grishin, Structural classification of zinc fingers: survey and summary, Nucleic Acids Res. 31 (2003) 532–550.
[19] T.E. Wolff, J.M. Berg, C. Warrick, K. Hodgson, R.H. Holm, The molybdenum–iron–sulfur cluster complex $[Mo_2Fe_6S_9(SC_2H_5)8]^{3-}$. A synthetic approach to the molybdenum site in nitrogenase, J. Am. Chem. Soc. 100 (1978) 4630.
[20] J.E. Pennerhahn, R.M. Fronko, V.L. Pecoraro, C.F. Yocum, S.D. Betts, N.R. Bowlby, Structural characterization of the manganese sites in the photosynthetic oxygen-evolving complex using X-ray absorption spectroscopy, J. Am. Chem. Soc. 112 (1990) 2549.
[21] K. Hayakawa, K. Hatada, P. D'Angelo, S. Della Longa, C.R. Natoli, M. Benfatto, Full quantitative multiple-scattering analysis of X-ray absorption spectra: application to potassium hexacyanoferrat(II) and -(III) complexes, J. Am. Chem. Soc. 126 (2004) 15618–15623.
[22] M. Benfatto, Z.Y. Wu, Multiple scattering approach to X-ray absorption spectroscopy, Nucl. Sci. Technol. 14 (2003) 9–19.
[23] K. Clark-Baldwin, D.L. Tierney, N. Govindaswamy, E.S. Gruff, C. Kim, J. Berg, S.A. Koch, J.E. Penner-Hahn, The limitations of X-ray absorption spectroscopy for determining the structure of zinc sites in proteins. When is a tetrathiolate not a tetrathiolate?, J Am. Chem. Soc. 120 (1998) 8401–8409.
[24] F.M. Wu, J.H. Zhang, J.P. Sun, H.D. Huang, P. Ji, W.S. Chu, M.J. Yu, F.F. Yang, Z.Y. Wu, J.H. Wu, Y.Y. Shi, Solution structure of human DESR1, a CSL zinc-binding protein, Proteins: Structure, Function, and Bioinformatics 71 (2008) 514–518.
[25] K.L. Borden, M.N. Boddy, J. Lally, N.J. O'Reilly, S. Martin, K. Howe, E. Solomon, P.S. Freemont, The solution structure of the RING finger domain from the acute promyelocytic leukaemia proto-oncoprotein PML, EMBO J. 14 (1995) 1532–1541.
[26] M. Benfatto, A. Congiu-Castellano, A. Daniele, S. Della Longa, MXAN: a new software procedure to perform geometrical fitting of experimental XANES spectra, J. Synchrotron Radiat. 8 (2001) 267.
[27] M. Benfatto, S. Della Longa, Y. Qin, Q. Li, G. Pan, Z. Wu, S. Morante, The role of Zn in the interplay among Langmuir–Blodgett multilayer and myelin basic protein: a quantitative analysis of XANES spectra, Biophys. Chem. 110 (2004) 191.
[28] P. Frank, M. Benfatto, R.K. Szilagyi, P. D'Angelo, S. Della Longa, K.O. Hodgson, The solution structure of $[Cu(aq)]^{2+}$ and its implications for rack-induced bonding in blue copper protein active sites, Inorg. Chem. 44 (2005) 1922.

[29] S. Li, Z. Zhou, W. Chu, W. Gong, M. Benfatto, T. Hu, Y. Xie, D. Xian, Z. Wu, Investigation of zinc-containing peptide deformylase from *Leptospira interrogans* by X-ray absorption near-edge spectroscopy, J. Synchrotron Radiat. 12 (2005) 111.
[30] W. Zhao, W.S. Chu, F.F. Yang, M.J. Yu, D.L. Chen, X.Y. Guo, D.W. Zhou, N. Shi, A. Marcelli, L.W. Niu, M.K. Teng, W.M. Gong, M. Benfatto, Z.Y. Wu, Quantitative investigation of two metallohydrolases by X-ray absorption spectroscopy near-edge spectroscopy nuclear instruments and methods in physics research section A: accelerators, spectrometers, Detect. Assoc. Equip. 580 (2007) 451–456.
[31] F.F. Yang, W.S. Chu, M.J. Yu, Y. Wang, S.X. Ma, Y.H. Dong, Z.Y. Wu, Local structure investigation of the active site of the imidazolonepropionase from Bacillus subtilis by XANES spectroscopy and *ab initio* calculations, J. Synchrotron Radiat. 15 (2008) 129–133.
[32] P. D'Angelo, M. Benfatto, S. Della Longa, N.V. Pavel, Combined XANES and EXAFS analysis of Co^{2+}, Ni^{2+}, and Zn^{2+} aqueous solutions, Phys. Rev. B 66 (2002) 064209.
[33] S.M. Webb, G.J. Dick, J.R. Bargar, B.M. Tebo, Evidence for the presence of Mn(III) intermediates in the bacterial oxidation of Mn(II), Proc. Natl. Acad. Sci. 102 (2005) 5558–5563.
[34] A. Pasquarello, I. Petri, P. Salmon, O. Parisel, R. Car, E. Toth, D.H. Powell, H.E. Fischer, L. Helm, A.E. Merbach, First solvation shell of the Cu(II) aqua ion: evidence for fivefold coordination, Science 291 (2001) 856–859.
[35] C.R. Natoli, M. Benfatto, EXAFS and Near Edge Structure IV, J. Phys. (Paris) Colloq. 47 (C8) (1986) 11.
[36] Z.Y. Wu, G. Ouvrard, S. Lemaux, P. Moreau, P. Gressier, F. Lemoigno, J. Rouxel, Sulfur K-edge X-ray-absorption study of the charge transfer upon lithium intercalation into titanium disulfide, Phys. Rev. Lett. 77 (1996) 2101.
[37] J.C. Fuggle, J.E. Inglesfield, Unoccupied Electronic States, Topics in Applied Physics, Appendix B, Springer, Berlin, 1992.
[38] O.M. Roscioni, P. D'Angelo, G. Chillemi, S. Della Longa, M. Benfatto, Quantitative analysis of XANES spectra of disordered systems based on molecular dynamics, J. Synchrotron Radiat. 12 (2005) 75–79.
[39] J.G. Norman, Non-empirical versus empirical choices for overlapping-sphere radii ratios in SCF-X^{α}-SW calculations on ClO_4^- and SO_2, Mol. Phys. 81 (1974) 1191–1198.
[40] Y. Joly, X-ray absorption near-edge structure calculations beyond the muffin-tin approximation, Phys. Rev. B 63 (2001) 125120.
[41] Z.Y. Wu, D.C. Xian, C.R. Natoli, A. Marcelli, A. Mottana, E. Paris, Symmetry dependence of X-ray absorption near-edge structure at the metal *K* edge of 3d transition metal compounds, Appl. Phys. Lett. 79 (2001) 1918–1920.
[42] M. Benfatto, P. D'Angelo, S. Della Longa, N.V. Pavel, Evidence of distorted fivefold coordination of the Cu^{2+} aqua ion from an X-ray-absorption spectroscopy quantitative analysis, Phys. Rev. B 65 (2002) 174205.
[43] K. Hayakawa, K. Hatada, C.R. Natoli, P. D'Angelo, S. Della Longa, M. Benfatto, A quantitative structural investigation of the XANES spectra of potassium ferrocyanide (III) at the iron K-edge, Phys. Scripta 115 (2005) 152–154.
[44] M. Benfatto, S. Della Longa, Geometrical fitting of experimental XANES spectra by a full multiple-scattering procedure, J. Synchrotron Radiat. 8 (2001) 1087.
[45] A. Arcovito, D.C. Lamb, G.U. Nienhaus, J.L. Hazemann, M. Benfatto, S. Della Longa, Light-induced relaxation of photolyzed carbonmonoxy myoglob: a temperature-dependent X-ray absorption near-edge structure (XANES) study, Biophys. J. 88 (2005) 2954–2964.